Journal of Ethnopharmacology 253 (2020) 112663

Contents lists available at ScienceDirect

Journal of Ethnopharmacology

journal homepage: www.elsevier.com/locate/jethpharm

Antipyretic and antitumor effects of a purified polysaccharide from aerial parts of *Tetrastigma hemsleyanum*

Bingqi Zhu[a,1], Chaodong Qian[b,1], Fangmei Zhou[a], Jingjing Guo[c], Nipi Chen[b], Chengxian Gao[b], Bo Jin[b], Zhishan Ding[a,*]

[a] College of Medical Technology, Zhejiang Chinese Medical University, Hangzhou, Zhejiang, 310053, China
[b] College of Life Science, Zhejiang Chinese Medical University, Hangzhou, 310053, Zhejiang, China
[c] Shaoxing Central Hospital, Shaoxing, Zhejiang, 312000, China

ARTICLE INFO

Keywords:
Tetrastigma hemsleyanum
Polysaccharide
Antipyretic activity
Antitumor activity
Cytokines
TLR4

ABSTRACT

Ethnopharmacological relevance: *Tetrastigma hemsleyanum* Diels et Gilg (Sanyeqing) is traditionally used as a folk medicine for the treatments of inflammation, high fever, hepatitis and cancer, and can improve the immune function of the patient. It belongs to the family of *Vitaceae*, and is mainly distributed in southeast China (Yunnan province) and can be found in India (Andaman Islands), Myanmar, Thailand, Vietnam, Malaysia and Indonesia in the valleys with 1100–1300 m above the sea level.

Aim of the study: The present study aimed to characterize the chemical properties of a purified polysaccharide extracted from the aerial part of *Tetrastigma hemsleyanum* (SYQP) and investigate its antipyretic and antitumor effects in mice models.

Materials and methods: Water-soluble crude polysaccharides from the aerial parts of *Tetrastigma hemsleyanum* were extracted and fractionated by DEAE and gel permeation chromatography. Homogeneity, molecular weight, monosaccharide composition, and FTIR analysis were performed to characterize the SYQP. Antipyretic effect of SYQP was examined using Brewer's yeast induced hyperthermia test. Antitumor effect was investigated using H22 tumor bearing mice. The serum cytokines were determined to evaluated the biological activities of SYQP.

Results: SYQP was composed of galacturonic acid (GalA), glucose (Glc), mannose (Man), arabinose (Ara), galactose (Gal), and rhamnose (Rha) with a molar ratio of 11.3:7.1:2.5:1.0:0.9:0.5 and it had an average molecular weight of 66.2 kDa. The oral administration of SYQP at 200 and 400 mg/kg could markedly suppress the hyperthermia of mice induced by Brewer's yeast and decrease the production of cytokines especially prostaglandin E2 (PGE2) in the serum of mice. SYQP inhibited the growth of H22 tumor in mice with inhibitory rate of 39.9% at the administration dose of 200 mg/kg and increased the production of cytokines such as tumor necrosis factor-alpha (TNF-a) and interferon γ (IFN-γ). Experimental results showed that the preventive administration of SYQP before lipopolysaccharide (LPS) reduced the high cytokine levels such as IL-6, IL-10 and IFN-γ, indicating that SYQP might act as a competitor with LPS to interact with toll like receptor 4 (TLR4), which further regulated the secretion of cytokines.

Conclusion: The anti-inflammatory and antitumor activities of SYQP might be related to its regulation of host immune function by controlling the secretion of cytokines.

List of compounds

Glucose, mannose, arabinose, galactose, rhamnose, trifluoroacetic acid, glucuronic acid, 3-(4,5-dimethylthiazol-2-yl)-5-(3-carboxymethoxyphenyl)-2-(4-sulfophenyl)-2H-tetrazolium inner salt, bicinchoninic acid, dextrans, ethanol, cyclophosphamide.

List of botanical varieties

Tetrastigma hemsleyanum, Stahlianthus involucratus, Ampelopsis megalophylla, Epimedium koreanum Nakai, Marsdenia tenacissima, Dendrobium devonianum, Phellinus igniarius.

* Corresponding author.
E-mail address: dzszjtcm@163.com (Z. Ding).
[1] The authors contributed equally.

https://doi.org/10.1016/j.jep.2020.112663
Received 15 September 2019; Received in revised form 20 January 2020; Accepted 7 February 2020
Available online 08 February 2020
0378-8741/

List of abbreviations

Glc	Glucose
Man	Mannose
Ara	Arabinose
Gal	Galactose
Rha	Rhamnose
GalA	Galacturonic acid
MTS	3-(4,5-dimethylthiazol-2-yl)-5-(3-carboxymethoxyphenyl)-2-(4-sulfophenyl)-2H-tetrazolium inner salt
ELISA	Enzyme-linked immunosorbent assay
TNF-α	Tumor necrosis factor-alpha
IL-6	Interleukin-6
IL-10	Interleukin-10
IL-12	Interleukin-12
IL-1β	Interleukin-1beta
cAMP	Cyclic adenosine monophosphate
IFN-γ	Interferon gamma
PGE2	Prostaglandin E2
WSP	Water soluble part
ESP	Ethanol soluble part
BCA	Bicinchoninic acid
HPGPC	High performance gel permeation chromatography
GC-MS	Gas chromatography mass spectrometry
FTIR	Fourier transform infrared spectroscopy
SYQP	A purified polysaccharide from aerial parts of *Tetrastigma hemsleyanum*
CTX	Cyclophosphamide
THP-1	Human acute monocytic leukemia cell line
RAW264.7	Abelson leukemia virus transformed monocyte/macrophage cell line
DMEM	Dulbecco's modified Eagle's medium
FBS	Fetal Bovine Serum
LPS	Lipopolysaccharide
SYQPR	Reduction product of SYQP
NSAID	Nonsteroidal anti-inflammatory drugs
TLR4	Toll-like receptor 4
PAMP	Pathogen-associated molecule pattern
MyD88	Myeloid differential protein-88
TRIF	Adaptor inducing interferon-β
MAPK	Mitogen-activated protein kinase
LBP	Lipopolysaccharide binding protein
NF-κB	Nuclear factor kappa-B

1. Introduction

Tetrastigma hemsleyanum Diels et Gilg, which is known as Sanyeqing in China, is a perennial herb native to China and its medicinal applications in clearing heat and promoting blood circulation were recorded firstly in book *Compendium of Materia Medica* by Li Shizhen in the 16th century (Guo et al., 2019). For centuries, the whole plant of Sanyeqing has been extensively used in traditional folk medicine to treat various diseases including high fever, infantile febrile convulsion, pneumonia and rheumatic arthritis and has been cited in *Flora of China* (Chu et al., 2019; Sun et al., 2013; Xiong et al., 2015). The wide widespread applications of Sanyeqing in antipyretics and anti-inflammatory were evidenced by modern pharmacological and clinical studies in febrile rats induced by active dry yeast and paw edema induced by carrageenin (Guo et al., 2019; Liu et al., 2016; Ye and Liu, 2015). In the past decades, an increasing number of cancer patients were treated by Sanyeqing for its antitumor effects to leukemia and carcinomas of the lung, liver, stomach and studies revealed that Sanyeqing can suppress the proliferation of tumor cells and induce apoptosis in various cancer cells (Feng et al., 2014; Sun et al., 2018; Xiong et al., 2015; Zhong et al., 2016). Both aerial parts and root tubers of Sanyeqing were clinically utilized and their antipyretic and antitumor effects were experimentally confirmed by studies (Guo et al., 2019; Sun et al., 2017, 2018; Wang et al., 2018; Xiong et al., 2015).

Various chemical components, such as flavonoids, phenolic acids and polysaccharides, have been confirmed as the main active constituents of Sanyeqing with the development of analytical methods (Wang et al., 2018; Ye and Liu, 2015). Many studies reported organic solvent extract of the Chinese folk medicine as the major part that exhibits biological activities (Xiong et al., 2015). As one of the important compounds that can be extract by ethanol, flavonoids obtained from Sanyeqing have been proved to be one of the major contents responsible for antitumor and antioxidant activities (Du et al., 2015; Feng et al., 2014; Ye and Liu, 2015). The phenolic compounds from ethanol extracts of Sanyeqing has been documented to be effective in antitumor and anti-inflammatory (Wang et al., 2018). Petroleum ether fraction of Sanyeqing had antitumor activity by inducing apoptosis in human cervical carcinoma HeLa cells (Xiong et al., 2015). However, the decoction of Sanyeqing using water was widely used in traditional folk medicine, and the active constituents from water extract of Sanyeqing, including polysaccharides, remained poorly investigated.

As one of the important water soluble components, polysaccharides are increasingly attracting attentions of researchers for their various biological functions and valuable pharmacological activities (Chen et al., 2019; Yu et al., 2018). The polysaccharides are high-molecular biomacromolecules isolated from natural resources, including plant, fungi and seaweed, and they have been proved to be effective in antitumor, immunomodulation, antioxidation and anti-inflammatory activities (Yu et al., 2018).Therefore, the bioactive polysaccharides have been used in biochemical and medical practical application and were recommended as promising functional food supplements (Huang et al., 2015; Yu et al., 2018). Reports revealed that the bioactivities of polysaccharides were closely related to their chemical properties (Liu et al., 2015b). Although several studies reported the antioxidant, antihyperlipidemic, antibacterial activities and hypoglycemic effects of polysaccharides extracted from Sanyeqing (Chen et al., 2019; Ru et al., 2019a; Ru et al., 2019b), limited report has been found in investigating the antipyretic and antitumor effects and the mechanisms remain unclear.

Additionally, most studies focused on the root tubers of Sanyeqing, and limited information on the polysaccharides extracted from aerial parts of Sanyeqing can be found (Xiong et al., 2015). Sanyeqing requires a three years long plantation before harvest, therefore, the effective use of the aerial part is meaningful in order to raise economic returns. Our preliminary study found that water extracts of aerial part of Sanyeqing exhibited good antipyretic activities. Since the polysaccharides were the main compounds of water extracts, the chemical and pharmacological investigations of polysaccharides are critical in studying the aerial parts of Sanyeqing.

This study aimed to extract and isolate a purified polysaccharide from aerial parts of Sanyeqing followed by characterization of its chemical properties. The antipyretic effect was evaluated by the yeast-induced hyperthermia mice models, and antitumor effects were investigated by H22 tumor bearing mice. Cytokines from the serum of mice were evaluated and their regulation mechanisms were studied.

2. Materials and methods

2.1. Materials and reagents

The aerial parts of Sanyeqing were provided by Hangzhou Sanri Agri-Tech Co., Ltd. (Hangzhou, China) and they were obtained in

March 2015 from a planting base in Xindeng, Zhejiang province, China. The plant was authenticated by professor Zhishan Ding from Zhejiang Chinese Medical University. The voucher specimens are deposited in the laboratory centre of medical technology college in Zhejiang Chinese Medical University in Hangzhou, China.

Glucose (Glc), mannose (Man), arabinose (Ara), galactose (Gal), rhamnose (Rha), trifluoroacetic acid (TFA), glucuronic acid, 3-(4,5-dimethylthiazol-2-yl)-5-(3-carboxymethoxyphenyl)-2-(4-sulfophenyl)-2H-tetrazolium inner salt (MTS), and dextrans with molecular weights of 5 kDa, 25 kDa, 50 kDa, 80 kDa, and 150 kDa were purchased from Merck (Darmstadt, Germany). BCA protein assay kit was obtained from Beyotime biotechnology (Shanghai, China). Enzyme-linked immunosorbent assay (ELISA) kits for tumor necrosis factor-alpha (TNF)-a, interleukin-6 (IL-6), IL-10, IL-12, cyclic adenosine monophosphate (cAMP), interferon gamma (IFN-γ), interleukin-1beta (IL-1β) and prostaglandin E2 (PGE2) were obtained from Shanghai Xinfan Biotechnology company (Shanghai, China). lipopolysaccharide (LPS) ELISA kit was purchased from Meimian Biotechnology (Yancheng, Jiangsu, China). Other reagents used in this study were of analytical grade and were obtained from Sinopharm chemical reagent Co. Ltd. (Shanghai, China) and Merck (Darmstadt, Germany). The water used in this study were de-ionized water obtained from a Merck Milli-Q water purification system (Darmstadt, Germany).

2.2. Animals

Healthy male Kunming mice (22 ± 2 g), ICR male mice (25 ± 2 g), and BALB/c male mice (22 ± 2 g) were purchased from the laboratory animal center of Zhejiang Chinese Medical University (Hangzhou, China). The mice were housed in Plexiglas cages at a temperature of 21–23 °C, a relative humidity of 30–70%, 12 h light/dark cycle, and had free access to food and water. All animals were cared for according to the National Institutes of Health (NIH) Guide for the Care and Use of Laboratory Animals. Formal approval to conduct the experiments was obtained from the Animal Subjects Review Board of Zhejiang Chinese Medical University.

2.3. Preparation and analysis of a polysaccharide from aerial parts of Sanyeqing

2.3.1. Extraction and purification of polysaccharide

The aerial parts of Sanyeqing was air-dried and powdered with a waring blender. 200 g plant powder was extracted by 1 L de-ionized water at 80 °C for 30 min and repeated three times. The water extract solutions were combined, filtered, centrifuged at 4000 rpm for 15 min before concentration under vacuum, and dried product was named as water soluble part (WSP). The concentrated solution was added with 95% ethanol solution of triploid volume and subsequently placed in an environment of 4 °C for 12 h to precipitate polysaccharides. After centrifugation, the precipitation was re-dissolved in water and the precipitation procedure was repeated. The freeze-dried precipitation was obtained as crude polysaccharides. To deproteinated crude polysaccharides, sevag method was applied by adding n-butyl alcohol:-chloroform (1:4,V/V) into water solution of polysaccharides and supernatant was collected after vigorously shaking and centrifugation at 4000 rpm for 10 min (Xu et al., 2019). The deproteinated sample was fractionated on a DEAE-Sepharose fast flow column (2.6 cm × 30 cm) and eluted with a stepwise gradient of 0.2, 0.5 and 1.0 mol/L NaCl solutions at a flow rate of 1.0 mL/min. The polysaccharide fraction eluted with 0.2 mol/L NaCl was further purified by a Superdex-200 (2.0 cm × 80 cm) chromatography column eluted with de-ionized water to obtain a purified polysaccharide, which was named as SYQP.

2.3.2. Homogeneity and molecular weight determination

The homogeneity and molecular weight of the obtained polysaccharide were determined by high-performance gel permeation chromatography (HPGPC) on a Waters Ultrahydrogel 500 column (Milford, MA, USA) using isocratic elution with 20 mmol/L ammonium acetate solution. HPGPC was performed on a Waters 1525 HPLC system equipped with an evaporative light scattering detector. The sample was dissolved in the mobile phase to prepare a solution of 1 mg/mL, and the injection volume was 20 μL. Dextrans standards with molecular weights of 5 kDa, 25 kDa, 50 kDa, 80 kDa, and 150 kDa were used as standard molecular markers.

2.3.3. Chemical property and monosaccharide composition analysis

Total neutral sugar content was determined by phenol–sulphuric acid colorimetry method (Dubois et al., 1956) where Glc was used as standard. Uronic acid content was assessed through the Blumenkrantz and Asboe-Hansen method (Blumenkrantz and Asboe-Hansen, 1973) where glucuronic acid was used as a standard. Protein concentration was determined with a BCA protein assay kit using bovine serum albumin as a standard.

Additionally, monosaccharide composition of the polysaccharide was determined using a gas chromatography mass spectrometry (GC-MS) according to the method in the literature (Zheng et al., 2016). After hydrolyzation of polysaccharides with TFA at 100 °C for 6 h in a sealed test tube, the hydrolysed products were evaporated to dryness with the addition of methanol to remove TFA. Deionized water and sodium tetrahydroborate ($NaBH_4$) were added successively to reduce the monosaccharide for 3 h. The reduced products were neutralized with acetic anhydride and evaporated to dry before acetylation with 3 mL of pyridine and 3 mL of acetic anhydride for 1 h incubation at 100 °C. After cooling to room temperature, excrescent acetic anhydride was removed by drying with a rotary evaporator. The acetylated derivatives were analysed by a Shimadzu GC-MS QP2010 system (Kyoto, Japan) equipped with an HP-5 capillary column (30.0 m × 0.25 mm, 0.25 μm). Column oven temperature was ramped from 120 °C to 200 °C with a rate of 2 °C/min and further increased to 250 °C with a rate of 10 °C/min. Heilium was used as carrier gas and the flow rate was set at 1.0 mL/min. The MS operating parameters were as follows: ionization energy, 70 eV; ion source temperature, 230 °C; data was collected in scan mode. Retention time and mass spectra were used to identify the compounds. The uronic acid in the sample was reduced to neutral (Shao et al., 2015) and subsequently determined by GC-MS.

2.3.4. Infrared spectral analysis

A Thermo Scientific Nicolet iS5 Fourier transform infrared (FTIR) spectrometer (Waltham, MA, USA) was used in the measurement and the dried sample was ground with potassium bromide powder and pressed into pellet for spectrometric measurement in the frequency range of 4000–450 cm^{-1}.

2.4. Antipyretic activity

Antipyretic activity was evaluated by Brewer's yeast-induced hyperthermia in mice as described previously (Pingsusaen et al., 2015; Teotino et al., 1963). Briefly, the base rectal temperature of each ICR male mouse was measured by a thermometer in rectum with a depth of 2 cm before the yeast injection. Mice with base rectal temperature of 36.5–37.5 °C were selected for antipyretic assays. Hyperthermia was induced by the administration of 20% aqueous suspension of yeast in saline subcutaneously with a dosage of 20 mL/kg body weight. 9 h after yeast injection, the rectal temperatures of the mice were recorded, and drugs were immediately administered to the mice at 0.8 °C above the base rectal temperature or higher. Drugs including aspirin (200 mg/kg body weight) and SYQP (200 and 400 mg/kg body weight) were administered orally, while saline (10 mL/kg) was used in control group. Rectal temperatures were measured at given time points after drug administration, and survival rates were recorded for 24 h.

2.5. Determination of serum cytokine levels

Blood samples were collected from orbital cavity after 2 h of drug administration to detect the serum cytokine levels in mice with yeast-induced hyperthermia. Serum was separated by centrifugation at 4000 r/min at 4 °C for 10 min and then stored at −80 °C until measurement of cytokines. The concentrations of soluble cytokines were determined using ELISA kits according to the manufacturer's protocols.

2.6. Antitumor activity

The antitumor effect of SYQP was evaluated in male Kunming mice as previously described (Xie et al., 2015). In brief, viable cancer cells (0.2 mL, 1 × 10^7 cells/mL) were transplanted subcutaneously into the right groins of the mice. After inoculation, tumor-bearing mice were randomly divided into five groups of 10 mice each as follows: control group treated with normal physiological saline, 50 mg/kg cyclophosphamide (CTX) group, and three SYQP groups administrated at 50, 100 and 200 mg/kg concentration levels. Normal physiological saline and SYQP were orally administered once daily for 10 consecutive days. CTX was injected intraperitoneally once every other day. Tumor volumes were measured in 4, 7 and 10 days after inoculation (Zhao et al., 2017). Exactly 12 h after the last administration, the mice were weighed and sacrificed by cervical dislocation. Blood samples were collected from orbital cavity for the detection of serum cytokines in mice as the described method in section 2.5. The tumors, spleens and thymuses were collected and weighted immediately. Tumor inhibitory rate, spleen index and thymus index were calculated by the following equation:

$$\text{Inhibitory rate}\,(\%) = \left(1 - \frac{\text{average tumor weight of tested group}}{\text{average tumor weight of control group}}\right) \times 100$$

$$\text{spleen index}\,(mg/g) = \frac{\text{spleen weight}\,(g)}{\text{mice weight}\,(g)} \times \frac{1000\,(mg)}{1\,(g)}$$

$$\text{thymus index}\,(mg/g) = \frac{\text{thymus weight}\,(g)}{\text{mice weight}\,(g)} \times \frac{1000\,(mg)}{1\,(g)}$$

2.7. Spleen lymphocyte proliferation assay

Splenocytes from mice were prepared and proliferated according to a previously described method (Lv et al., 2014), which had been modified for the MTS assay. In brief, splenocytes were cultured in 96-well plates (1 × 10^6 cells/well) in RPMI and incubated with SYQP at 0–400 μg/mL for 48 h. Subsequently, 40 μL MTS was added to each well, and the cells were incubated for an additional 2 h. The absorbance at 490 nm was recorded.

2.8. Measurement of cytokines secreted by THP-1 and RAW264.7 cells

THP-1 and RAW 264.7 cells were purchased from Shanghai Institute for Biological Sciences, Chinese Academy of Sciences. They were cultured in Dulbecco's modified Eagle's medium (DMEM) supplemented with 10% heat-inactivated FBS, 100 U/ml penicillin and 100 μg/ml streptomycin. The media were replaced every 2–3 days.

THP-1 cells were seeded into a 96-well plate (5 × 10^4 cells/well) and cultured for 48 h. Then, TAK-242 at four different concentrations levels of 0, 5, 10 and 20 μg/mL were prepared to incubate THP-1 cells for 3 h before adding LPS or SYQP. LPS and SYQP were added to a final concentration of SYQP at 100 μg/mL, and LPS at 100 ng/mL and 1 μg/mL. After incubation for 24 h, the cultured supernatants were collected. RAW264.7 cells were seeded into another 96-well plate (1 × 10^5 cells/well) and same procedures as THP-1 cultivation were repeated. The quantifications of cytokines TNF-α and IP-10 were determined using commercial ELISA kits.

2.9. LPS induced inflammatory cytokines measurement

Healthy BALB/c male mice were selected and divided into 5 groups. Normal group were treated with normal physiological saline. SYQP i.g. group was administrated intragastrically (i.g.) with 150 mg/kg SYQP

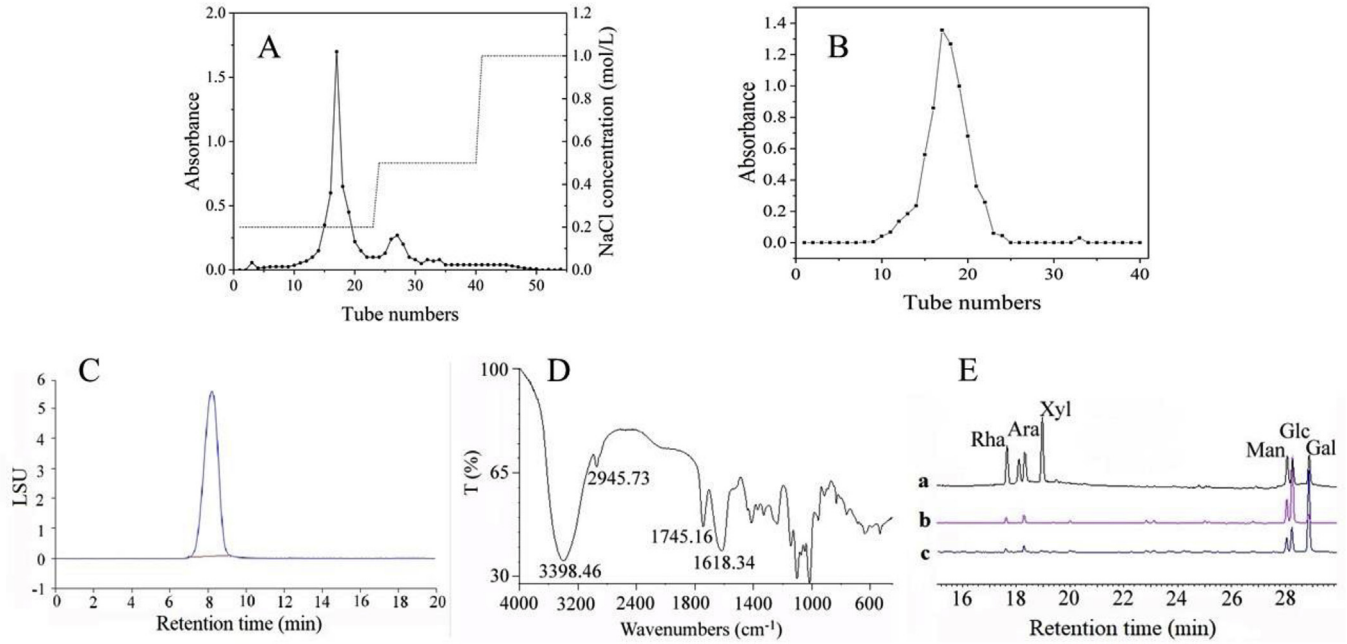

Fig. 1. Isolation and characterization of the polysaccharide (A) anion-exchange chromatogram of crude polysaccharides on DEAE-Sepharose fast flow column, 10 mL eluents were collected in each tube and absorbance was measured at 490 nm; (B) gel chromatographic profile on Superdex-200 column, 10 mL eluents were collected in each tube and absorbance was measured at 490 nm; (C) HPGPC chromatogram of SYQP; (D) FT-IR spectrum of SYQP; (E) GC-MS total ion chromatogram of monosaccharides in samples: (a) monosaccharides standards, (b) SYQP, and (c) SYQPR.

for 2 consecutive days. SYQP i.p. group and SYQP + LPS group were administrated daily by intraperitoneal (i.p.) injection with 150 mg/kg SYQP for 2 consecutive days. 2 h after the last administration, the SYQP + LPS group was intraperitoneally injected with 30 mg/kg LPS. LPS group and LPS + SYQP group were intraperitoneally injected with 30 mg/kg LPS, while the latter was further administrated with 150 mg/kg SYQP for two times in 10 min and 2 h. Exactly 6 h after the last administration for each group, blood samples were collected from orbital cavity for the detection of serum cytokine levels in mice as the described method in section 2.5.

2.10. Statistical analysis

Statistical analysis was performed using SPSS 19.0 software package (SPSS Inc., Chicago, IL, USA). Data were analysed using a one-way ANOVA. A value of $p < 0.05$ was considered statistically significant.

3. Results and discussion

3.1. Isolation and characterization of the polysaccharide

A total amount of 23.8 g WSP were obtained from 200 g Sanyeqing aerial part sample. After deproteination by sevag method, separation and purification were carried out by anion-exchange chromatography on a DEAE Sepharose column. A relatively strong peak was observed in the fraction eluted by 0.2 mol/L NaCl solution as shown in Fig. 1A, which was collected for further purification, while the fraction eluted with 0.5 mol/L NaCl solution presented a relatively weak peak and was discarded. The collected eluent was subsequently chromatographed on a Superdex-200 column, and one single peak was obtained as demonstrated in Fig. 1B. This fraction was collected and named SYQP for further analysis.

The homogeneity of SYQP was determined by HPGPC. As shown in Fig. 1 C, SYQP showed a symmetrical and narrow peak with a retention of 8.217 min, indicating it was a homogeneous polysaccharide. The calibration curve of dextran was lg Mw = 9.9008–0.6182t (R^2 = 0.9927), where Mw was molecular weight and t was retention time. Based on the calibration curve, the averages molecular weight of SYQP was approximately 66.2 kDa, which was relatively close with one of previous study (Ru et al., 2019b).

The total sugar and uronic acid contents of SYQP were determined as 83.3% and 48.9%, respectively. The protein contents of SYQP were determined as 4.54% with a BCA protein assay kit. Furthermore, the monosaccharide composition of SYQP was determined using GC-MS after being hydrolysed and derivatised. As shown in the chromatogram b of Fig. 1D, Glc, Man, Ara, Gal and Rha with relative molar ratio of 7.1:2.5:1.0:0.9:0.5 were observed in the SYQP hydrolysate. The carboxyl of uronic acid in SYQP was reduced to primary alcohol to determine the type of uronic acid. GC-MS results demonstrated that the reduction product (SYQPR) was composed of Glc, Man, Ara, Gal and Rha with a molar ratio of 7.2:2.4:1.0:12.2:0.5, as shown in the chromatogram c of Fig. 1D. The molar ratio of Gal increased more considerably in the hydrolysate of SYQPR compared with Ara. The proportions of other monosaccharides showed relatively small changes. Thus, the uronic acid in SYQP was mainly galacturonic acid (GalA) and the polysaccharide was mainly composed of GalA, Glc, Man, Ara, Gal and Rha with molar ratios of 11.3:7.1:2.5:1.0:0.9:0.5. From the above results, the uronic result obtained from GC-MS analysis agreed with the uronic acid measurement, and our purified polysaccharides shared a relative close molar ratio of Man, Ara and Rha with a previous study but much higher percentages of Glc and GalA (Ru et al., 2019a).

The FT-IR spectrum of SYQP is shown in Fig. 1C. Two characteristic absorptions of polysaccharides were observed at 3398.46 cm^{-1} and 2945.73 cm^{-1}, which corresponded to O–H stretching of carbohydrates and C–H stretching of the aromatic structures and the methyl group, respectively (Timilsena et al., 2016). A Strong absorption at 1618.34 cm^{-1} indicated the presence of carboxyl groups in SYQP. The peak at 1745.16 cm^{-1} suggested the presence of uronic acid (Ru et al., 2019b), which is consistent with the existence of GalA obtained from chemical analysis. The relative weak absorption bands around 1400 - 1300 cm^{-1} corresponded to the vibrations of C–H (Liu et al., 2015a). Three distinct bands around 1100 - 1000 cm^{-1} corresponded to the C–O stretching vibrations (Ru et al., 2019b), and might indicate the presence of pyranoside (Chen et al., 2019). In addition, the weak band near 900 cm^{-1} suggested the possible presence of the β-type glycoside (Chen et al., 2019; Ru et al., 2019b).

3.2. Antipyretic activity

In preliminary study of Sanyeqing, experiments were conducted to compare the WSP and ethanol soluble parts (ESP). WSP was prepared according to the method described in section 2.3.1 and ESP were prepared by the same method except using 95% ethanol as the extraction solvent. After concentration and freeze-drying, the powdered WSP and ESP were used to evaluate antipyretic activity by Brewer's yeast induced hyperthermia in mice. As demonstrated in Table 1, the temperature of the groups treated by ESP did not exhibited any significant change comparing with control group in 180 min ($P > 0.05$), implying no antipyretic effect. By contrast, the WSP exerted significant effects against yeast-induced hyperthermia by presenting significant temperature change ($P < 0.01$) comparing with control group after the administration of 20 g/kg WSP to mice. Therefore, the experimental results showed that WSP, which included polysaccharides, was effective in antipyretic caused by yeast in mice.

The phenolic compounds obtained from ESP of Sanyeqing had been reported for its antioxidant activity (Sun et al., 2017), and the presences phytosterol from ESP could induces apoptosis in human cervical carcinoma HeLa cells (Xiong et al., 2015). However, no literature has been found for ESP's antipyretic activity. It was reported that ethanol extract of *Stahlianthus involucratus* rhizome, which has long been used in

Table 1
Effects of Sanyeqing extracts on yeast-induced hyperthermia in mice.

Group	Dose	Rectal temperature (°C)				
	(g/kg)	Initial	Pyretic	60 min	120 min	180 min
Control	–	37.22 ± 0.23	38.30 ± 0.37	38.05 ± 0.31	37.92 ± 0.35	37.98 ± 0.32
Aspirin	0.2	37.22 ± 0.29	38.25 ± 0.34	36.46 ± 0.39[b]	36.47 ± 0.40[b]	36.22 ± 0.49[b]
WSP	5	37.16 ± 0.37	38.16 ± 0.28	37.39 ± 0.32[b]	37.45 ± 0.43	37.42 ± 0.39[a]
WSP	20	37.14 ± 0.39	38.21 ± 0.32	37.16 ± 0.34[b]	37.24 ± 0.38[b]	37.31 ± 0.37[b]
ESP	5	37.12 ± 0.32	38.27 ± 0.36	38.09 ± 0.44	37.83 ± 0.41	37.73 ± 0.28
ESP	20	37.21 ± 0.30	38.22 ± 0.40	37.86 ± 0.46	37.84 ± 0.42	37.74 ± 0.47

Results are represented as means ± SD ($n = 10$).
[a] Indicated significant difference from control group, $P < 0.05$.
[b] Indicated very significant difference from control group, $P < 0.01$.

traditional medicine to treat inflammation and fever, possess no antipyretic activity (Pingsusaen et al., 2015). Our result showed that ESP failed to reduce the temperature of the pyretic mice induced by yeast, while the WSP was found to be effective. The antipyretic activity might be due to the existent of polysaccharides, which is the main component of the WSP.

To further investigate the antipyretic effect of polysaccharide. WSP was further purified according the method in section 2.3.1 to obtain SYQP. The effect of SYQP on yeast-induced hyperthermia in mice is presented in Table 2. The rectal temperatures of the mice were rapidly reduced 60 min after the oral administration of 200 and 400 mg/kg of SYQP. The rectal temperature measured at 120 min and 180 min followed a trend of decline as the increment of time. Similar results were obtained in mice treated with aspirin at 200 mg/kg.

Although the hyperthermia temperature was reduced, the mice injected with dried yeast began to die in 5 h after drug administration subjected to a lethal dose of yeast. 100% of the tested mice treated with saline and aspirin died after 24 h as demonstrated in Fig. 2. However, 10% and 40% survival rate were observed when mice were treated with 0.2 and 0.4 g/kg SYQP, respectively. The results suggested that treatment with SYQP increased the survival counts compared with model and aspirin group within 24 h.

3.3. Effect of SYQP on serum cytokine levels in yeast induced hyperthermia mice

Yeast-induced pyrexia is a kind of pathogenic hyperthermia, which is an adaptive response of the host to an invading noxae (Ataŏglu et al., 2000). Foreign antigens stimulate the production of endogenous pyrogenic cytokines, and followed by increased blood plasma levels of TNF-a, IL-1β and IL-6 and activation of inflammatory transcription factors in the hypothalamus and circumventricular organs (Pingsusaen et al., 2015; Roy et al., 2019). Subsequently, the increased hypothalamic mRNA expression of TNF-α, IL-1β and IL-6 promote the synthesis of PGE2 and trigger a febrile response (Dangarembizi et al., 2018).

To investigate the antipyretic effects of SYQP on serum cytokine levels, serum was collected from mice with yeast-induced fever after 2 h of drug administration, and cytokines were determined by ELISA. As shown in Table 3, the levels of TNF-a, IL-1β, IL-6, cAMP and PGE2 in serum were more significantly increased in the control group compared with the normal group ($P < 0.05$). After oral administration of SYQP, all cytokine levels were reduced at 100, 200 and 400 mg/kg in a dose-dependent manner. Although the changes were less dramatic in IL-1β and TNF-α, whose significant differences showed in the highest dose at 400 mg/kg ($P < 0.05$), the concentration of PGE2, cAMP and IL-6 in serum were significantly reduced in all SYQP treated groups ($P < 0.05$). As one of the nonsteroidal anti-inflammatory drugs (NSAIDs), aspirin significantly reduced PGE2, IL-1β and TNF-α in the serum of mice induced with yeast hyperthermia, and its antipyretic effect could results from the inhibition of PGs synthesis within hypothalamus (Pingsusaen et al., 2015).

The capsule polysaccharides and proteins of fungi were the main

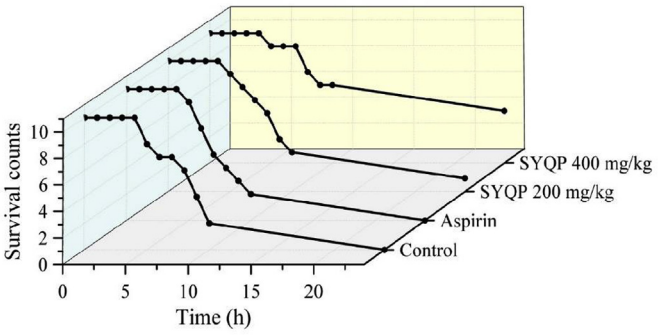

Fig. 2. Survival count of mice after yeast-induced hyperthermia. Mice were orally administered with SYQP at 400 mg/kg, 200 mg/kg, aspirin at 200 mg/kg, and physiological saline. ($n = 10$ per group).

causes of yeast induced hyperthermia. The ulceration at the yeast injection site induces a severe inflammatory response throughout the body, resulting in high fever. As a most commonly used thermogenic model, yeast can simulate fever under pathological conditions. In this model, body temperature increases rapidly, and maintains a high fever level for a long time with obvious inflammatory symptoms. Therefore, it is suitable for the pharmacological study of antipyretic or anti-inflammatory drugs. It was reported that treatment with *Ganoderma lucidum* polysaccharides could attenuate the increases of TNF-α and IL-1β in common carp with carbon tetrachloride-induced hepatocyte damage (Liu et al., 2015c), and *astragalus* polysaccharide reduces serum concentrations of cytokines including TNF-α and IL-1β in adjuvant-induced arthritic rats (Jin et al., 2012). As a result, significantly reduced levels of serum cytokines suggested that the antipyretic effect of SYQP was correlated with the inhibited release of pyrogenic cytokines.

3.4. Antitumor activities of SYQP

Cancers of the liver was one of the most commonly diagnosed in all cancer cases and was identified as a leading cause of cancer death all over the world (Chen et al., 2016). Searching for efficient drugs has been a vital task for decades. Polysaccharides are naturally occurring products and is currently attracting considerable attention because of their antitumor activities without significant side effects (Jiao et al., 2016). To investigate the medical application of Sanyeqing and bioactivities of its polysaccharides, mice bearing implanted H22 tumor were involved in this study. SYQP was administered to mice bearing implanted H22 tumor via oral gavage to evaluate its antitumor activity. After the last administration, the body weights of the mice were 36.73 g ± 2.54 g, 32.70 g ± 1.51 g, 34.55 g ± 2.81g, 34.65 g ± 2.47 g and 34.33 g ± 1.96 g for the control group, CTX group, 50 mg/kg SYQP group, 100 mg/kg SYQP group and 200 mg/kg SYQP group, respectively. As shown in Fig. 3 C, the tumor volumes of the mice treated with CTX and SYQP in 4, 7 and 10 days after inoculation were smaller than the control group. Larger decrements were

Table 2
Effects of SYQP on yeast-induced hyperthermia in mice.

Group	Dose	Body temperature (°C)				
	(mg/kg)	Initial	Pyretic	60 min	120 min	180 min
Control	–	37.11 ± 0.50	38.30 ± 0.31	38.51 ± 0.41	38.46 ± 0.37	38.24 ± 0.42
Asprin	200	37.24 ± 0.56	38.16 ± 0.22	36.91 ± 0.38**	36.33 ± 0.34**	35.90 ± 0.66**
SYQP	200	37.23 ± 0.39	38.27 ± 0.37	37.78 ± 0.42**	37.67 ± 0.47**	37.41 ± 0.37**
SYQP	400	37.30 ± 0.44	38.24 ± 0.31	37.64 ± 0.39**	37.53 ± 0.39**	37.35 ± 0.35**

Results are represented as means ± SD ($n = 10$).
* indicated significant difference from control group, $P < 0.05$.
**Indicated very significant difference from control group, $P < 0.01$.

Table 3
Effects of SYQP on serum cytokines in mice with yeast-induced hyperthermia.

Group	Dose (mg/kg)	PGE2 (ng/L)	IL-1β (ng/L)	cAMP (pg/mL)	IL-6 (pg/mL)	TNF-α (ng/L)
Normal	–	145.80 ± 24.42	8.90 ± 2.37	59.44 ± 6.03	27.39 ± 1.68	170.78 ± 27.86
Control	–	175.52 ± 19.24[b]	16.93 ± 3.45[b]	107.34 ± 13.12[b]	32.22 ± 1.93[a]	214.96 ± 31.76[a]
Aspirin	200	126.84 ± 45.48[d]	12.63 ± 3.57	101.44 ± 20.09	29.45 ± 2.62	153.86 ± 35.21[d]
SYQP	100	141.45 ± 16.45[c]	13.60 ± 3.40	81.15 ± 8.11[d]	26.85 ± 3.81[d]	196.70 ± 32.48
SYQP	200	131.90 ± 14.15[d]	12.51 ± 3.82	74.52 ± 7.21[d]	27.19 ± 4.54[c]	176.17 ± 27.94
SYQP	400	119.89 ± 24.87[d]	10.89 ± 3.03[c]	67.56 ± 8.47[d]	25.75 ± 3.54[d]	154.09 ± 20.28[d]

Results are represented as means ± SD (n = 10).
[a] Indicated significant difference from normal group, $P < 0.05$.
[b] Indicated very significant difference from normal group, $P < 0.01$.
[c] Indicated significant difference from control group, $P < 0.05$.
[d] Indicated very significant difference from control group, $P < 0.01$.

observed for the mice administrated with larger amounts of SYQP among the different SYQP treatment groups, and the CTX treatment exhibited the most significant inhibition of the tumor volume among all groups. The results provided inhibitory effects of SYQP to both the tumor size and weight in H22 tumor-bearing mice. The inhibition rate of H22 tumor were 39.9% at the dose of 200 mg/kg and showed a very significant differences comparing with control group with $P < 0.01$. Based on the experimental results, SYQP inhibited the tumor growth by exhibiting significant difference from control group and the inhibition rate increased with a larger administration dose of SYQP. CTX showed more potent antitumor effects than SYQP on the tumor growth with an inhibition rate of 66.5% to H22 tumor.

Thymus and spleen are important immune organs of animals, which play crucial roles in the production of immune cells and immune responses (Zong et al., 2018). To investigate the effect of SYQP to immune system *in vivo*, spleen index and thymus index were investigated. The results showed that both the thymus and spleen indexes were decreased significantly ($P < 0.01$) in the CTX group compared with control group, which means CTX inhibited the immune capacity of body and resulted in weakened immunity. The spleen and thymus indexes were improved comparing with control group and significant differences ($P < 0.01$) were observed when SYQP were treated at the dosage of 200 mg/kg. These data suggested that SYQP had a beneficial effect on immune organ in H22 tumor-bearing mice, which agreed with previous reports (Fan et al., 2018; Jiang et al., 2016).

Based on the result of the immune promoting effect in animal experiment, a further study was conducted to investigate the proliferation of splenocytes cultured with SYQP. Splenocytes were isolated from mice and cultured with SYQP. As shown in Fig. 3, the treatment of SYQP at 0, 50, 100, 200, 400 μg/mL significantly stimulated the

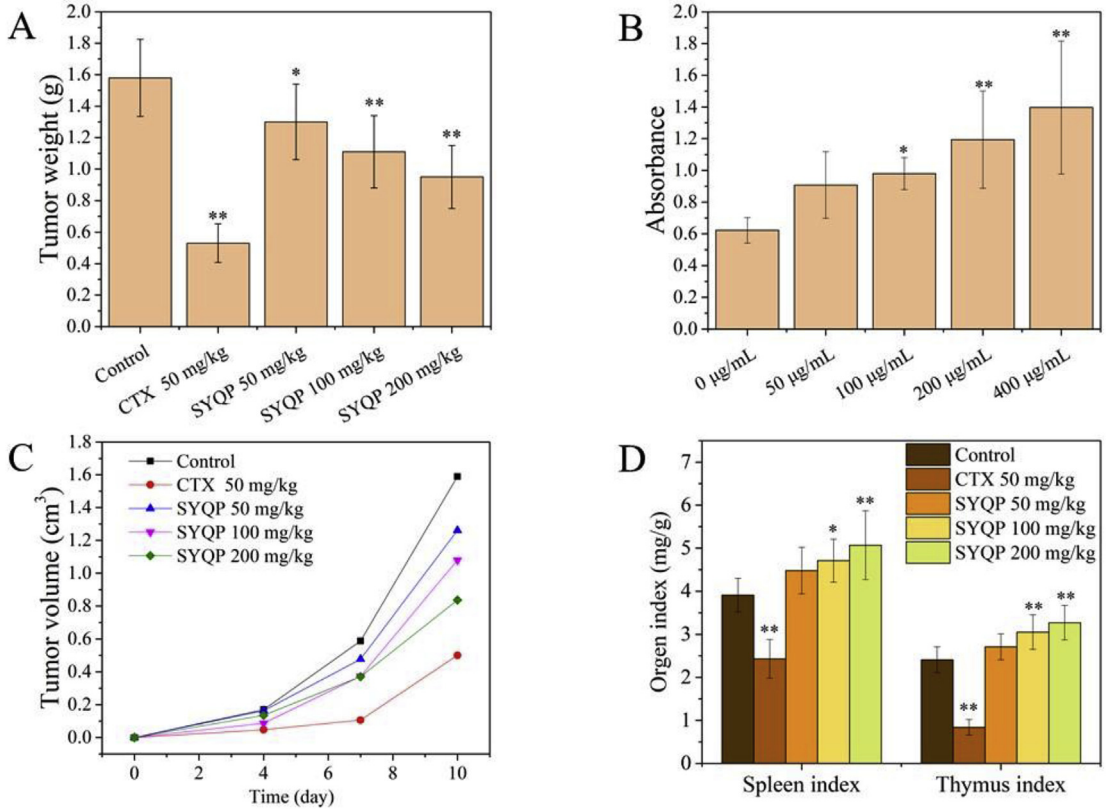

Fig. 3. Effects of SYQP on tumor growth, organ index and splenocyte proliferation. (A) Effect of SYQP on tumor growth in mice bearing H22 tumor. Average tumor weight (mean ± SD) were presented in each group (n = 10). (B) Effect of SYQP on splenocyte proliferation. Splenocytes were treated with indicated concentrations of SYQP for 48 h. Cell proliferation was determined using MTS method (n = 10); (C) Mean tumor volumes of the mice bearing H22 tumor; (D) Effects of SYQP on spleen index and thymus index. *indicated significant difference from control group, $P < 0.05$; **indicated very significant difference from control group, $P < 0.01$.

proliferation of splenocytes in a dose-dependent manner. Analogously, this treatment can promote mitogen-stimulated splenocyte proliferation, and significant differences were obtained when high concentrations of SYQP at 200 μg/mL and 400 μg/mL were applied. Identical results were obtained in other studies showing the polysaccharides extracted from *Ampelopsis megalophylla* could markedly enhance splenocyte proliferation (Xie et al., 2015). The splenocyte proliferation has been frequently used as an indicator of immunomodulation, and T and B lymphocytes are two important classes of immunological active cells (Xie et al., 2015), which are important in the regulation of the immune response (Liu et al., 2018). Previous studies indicated that the splenic lymphocyte proliferation was significantly depressed in tumor-bearing mammals (Zheng et al., 2015) and the stimulated proliferation of splenocytes in our study proved the beneficial effect of SYQP in immunomodulation. Therefore, the result obtained in this study implied that SYQP could potentially enhance both cellular and humoral immunity (Liu et al., 2018).

The precise antitumor mechanism of polysaccharide is considerably complex, and one mode of action by which polysaccharide exerts anticancer or antitumor activities might be the activation of host immune response (Meng et al., 2016; Wang et al., 2016). Both the tumor-bearing mice intragastrically administrated with SYQP and proliferation of splenocytes cultured with SYQP proved the positive effect of SYQP in up-regulation the immune system *in vivo* and *in vitro*, which possibly correlated with the inhibitory effect on tumor growth (Wang et al., 2017). Analogous phenomenon *in vivo* and *in vitro* have been observed in studies of polysaccharides obtained from *Epimedium koreanum* Nakai (Wang et al., 2017) and *Marsdenia tenacissima* (Jiang et al., 2016). The effect of SYQP on cytokines levels in tumor-bearing mice were further conducted to understand the mechanism of Sanyeqing treatment.

3.5. Effect of SYQP on serum cytokine levels in tumor-bearing mice

To investigate the antitumor effects of SYQP on serum cytokine levels. Serum samples were collected and cytokines were determined by ELISA method describe in section 2.5. When the tumors of the control group were heavier than 1 g, the eyes of the mice were removed and serum samples were collected after fasting for 12 h. Although the significant difference was hardly found between the normal group and control group, INF-γ, TNF-α and IL-6 levels were significantly increased in serum of tumor-bearing mice treated with 100 and 200 mg/kg SYQP compared with the control group ($P < 0.05$). No significant difference was observed for IL-1β among groups as shown in Table 4.

Cytokines, such as TNF-α and IFN-γ, which can be secreted by activated macrophages, plays an pivotal role in the development of immune responses (Xie et al., 2015). For example, TNF-α is important in host defense and can induce the expression of a number of other immunoregulatory and inflammatory mediators to inhibit the growth of tumor (Baugh and Bucala, 2001); IFN-γ induces the generation of T-cells and activates macrophages, which inhibits the proliferation of tumor (Xie et al., 2015). Moreover, SYQP treatment at concentrations of 10, 100 and 1000 μg/mL showed no significant effect on the growth of H22 hepatocarcinoma cell lines *in vitro*.

Among three possible mechanisms related to the antitumor activities, which included the inducing the apoptosis of tumor cells, improvement the immune function of the host and synergistic effect with traditional chemotherapy drugs (Yu et al., 2018), our results suggested that antitumor activities of SYQP were not achieved by killing tumor cells directly, but related to its immunoregulatory activity. The administration of Sanyeqing polysaccharides could activate immune function including macrophages, T or B lymphocytes and natural killer cells, and promote production of cytokines to facilitate regulation of the immune system (Yu et al., 2018). Previous report revealed that uronic acid in the polysaccharides played an important role in influencing the antitumor activity (Jin et al., 2017). Our result showed the existence of a high content of the GalA in SYQP, therefore, GalA may play one of the important roles in antitumor and regulating immunoregulatory activities besides other compositions. The bioactivity and pharmacology of GalA required a further investigation.

3.6. Binding of the SYQP to toll-like receptor 4 (TLR4) activates the immunomodulatory

TLRs are able to detect and signal in response to specific conserved motifs associated with microbial activity such as LPS (Tian et al., 2019). TLR4, which is critical in inflammatory responses, is important receptors on the surface of macrophages, and its activation by ligand may induce a rapid and extensive immune response via recognizing pathogen-associated molecule pattern (PAMP). As demonstrated in Fig. 4, The MyD88-dependent and TRIF-dependent (MyD88 independent) are two main signal pathways of TLR4, which can further activate nuclear factor kappa-B (NF-κB), thereby respectively regulating the production of proinflammatory cytokines, such as TNF-α, IL-6, IL-1β and IL-12, and interferons such as IP-10 and IFN-β (Long et al., 2018; Tian et al., 2019; Wang et al., 2019). The complexes of LPS and lipopolysaccharide binding protein (LBP) can bind with CD14, a differentiation antigen of monocytes, and then activate TLR4, which finally resulted as the promotion of the synthesis and secretion of cytokines (Wang et al., 2019; Wright et al., 1990). LPS can stimulate the immune system and strengthen the innate immune function when the concentration is low, however, high concentrations can cause extensive and intense inflammatory reactions, releasing mediators such as TNF-α, IL-6, IL-1β, NO, histamine, and oxygen free radicals, leading to a series of pathophysiological reactions, such as fever, severe infection, septic shock, multiple organ failure and diffuse intravascular coagulation.

Detection of LPS in SYQP were conducted according to the manufacturer's instruction and LPS was not detected in SYQP, which eliminated the possibility of the LPS contamination in SYQP. As demonstrated in Fig. 5, our study found that both SYQP at 100 μg/mL and LPS at 1 μg/mL and 100 ng/mL could stimulate THP-1 to secrete TNF-α and IP-10, which were significantly inhibited after the blockade of TLR4 by TAK-242. Same phenomenon was observed in RAW264.7, indicating

Table 4
Effect of SYQP on serum cytokines in mice bearing implanted H22 hepatocellular tumors.

Group	Dose (mg/kg)	TNF-α (ng/L)	IL-6 (pg/mL)	IFN-γ (ng/L)	IL-1β (ng/L)
Normal	–	377.07 ± 23.10	21.79 ± 4.19	34.88 ± 7.44	15.68 ± 2.01
Control	–	332.40 ± 27.59**	16.81 ± 4.81	36.29 ± 8.73	14.66 ± 1.56
SYQP	50	355.07 ± 37.21	21.32 ± 4.82	48.75 ± 12.38	12.97 ± 1.56
SYQP	100	371.07 ± 24.83△	23.65 ± 5.59△	53.64 ± 11.89*△	14.83 ± 2.56
SYQP	200	395.07 ± 20.49△△	26.11 ± 6.32△△	71.98 ± 17.99**△△	17.52 ± 5.23

Results are represented as means ± SD ($n = 10$).
*Indicated significant difference from normal group, $P < 0.05$;
**Indicated very significant difference from normal group, $P < 0.01$;
△Indicated significant difference from control group, $P < 0.05$;
△△Indicated very significant difference from control group, $P < 0.01$.

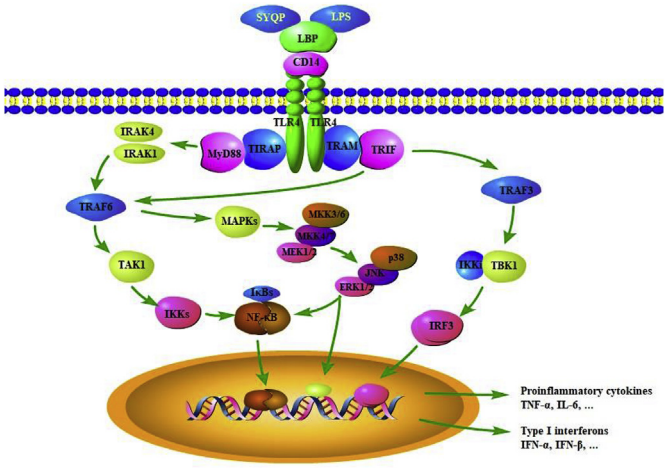

Fig. 4. The proposed mechanism underlying the immunoregulation effects of SYQP.

that SYQP can stimulate TLR4 via both MyD88-dependent and TRIF-dependent pathways, which might be identical with the mechanism of LPS. Similar results were obtained for the polysaccharides obtained from *Dendrobium devonianum* and *Phellinus Igniarius*, which demonstrated that both the polysaccharides and LPS can activated the TLR4 pathways followed by the secretion of the cytokines (Hu et al., 2020; Wang et al., 2019; Wu et al., 2019).

Animal study was carried out to investigate the serum inflammatory cytokines of LPS inflammatory model. The serum was collected and the cytokines were measured in 6 h after treatment. Based on the results of Table 5, the serum levels of inflammatory cytokines in both of SYQP i.g. group and SYQP i.p. group increased, indicating an up regulated effect of SYQP to the serum cytokines levels of LPS induced mice. Intraperitoneal injection of SYQP provided higher values than intragastrical administration. Distinct differences were found for the IL-6, IL-10 and TNF-α between the SYQP i.p. and SYQP i.g. groups, while relatively close values were obtained for IFN-γ and IL-12. The intraperitoneal injection of SYQP provided a more intense stimulation than intragastrically administration, which may attribute to the digestive system that partially degrade the SYQP or reduce the absorbing rate of SYQP. Compared with the normal group, serum levels of inflammatory cytokines related to TLR4 pathway, such as IL-6, IL-10, INF-γ, TNF-α and IL-12, increased dramatically after intraperitoneal injection of 30 mg/kg LPS into mice for 6 h ($P < 0.05, 0.01$) as demonstrated in Table 5. The serum IL-6, IL-10 and IL-12 content in the SYQP i.p. group was significantly higher than that in the normal group ($P < 0.01$). Compared with LPS group, SYQP pre-administration before LPS significantly inhibited the high levels of IL-6, IL-10 and INF-γ in serum ($P < 0.01$). The levels of other inflammatory cytokines were lower than those of LPS group, though there was no statistically significant difference. Meanwhile, in the post-administration of SYQP group, the expression level of INF-γ in serum was also decreased after the administration of SYQP, which was significantly different from that of LPS group ($P < 0.01$). Therefore, both pre- and post-administration of SYQP can effectively inhibit the expression of high levels of LPS-induced inflammatory cytokines. These results suggest that SYQP alone can weakly activate the TLR4 signalling pathway, and mildly stimulate the inflammatory response. We speculated that the interaction of SYQP with TLR4 can prevent LPS from binding to TLR4 and avoid severe inflammatory reaction caused by LPS. Other studies reported that polysaccharides, as an immunopotentiator, can inhibit LPS-induced inflammation via inhibiting TLR4/NF-κB signaling pathway (Zhao et al., 2019), which conformed our experimental results. Additionally, 24 h after intraperitoneal injection of 30 mg/kg LPS, all mice died with a mortality rate of 100%. SYQP administration before and after LSP injection can significantly improve the survival rate of mice from 0% to 50% and 40% at 48 h respectively. Therefore, preventive administration was better than therapeutic administration.

Based on the result of this study, we speculated that the SYQP played the role of the competitor with LPS in interacting with TLR4, and regulated the secretion of the cytokines, which reduced the body temperature in induced hyperthermia. On the other hand, the significant rise of serum cytokines in tumor-bearing mice predicted that SYQP may interact with TLR4 and promote the immune system via increasing the expression of correlated cytokines.

4. Conclusions

In this study, WSP and ESP from aerial parts of Sanyeqing were compared and ESP exhibited no antipyretic activities. SYQP, a purified polysaccharide was prepared, and a high content of GalA was found. Results of pharmacological tests indicated that SYQP exhibited good antipyretic activities in reducing the hyperthermia temperature of the mice induced by Brew's yeast and improved the survival of the mice subjected to a lethal dose of yeast. Serum levels of TNF-a, IL-1β and IL-6 was evaluated to investigate serum cytokine levels and significant decrease of PGE2 was observed after the administration of SYQP, indicating the mechanism of the antipyretic was resulted from the inhibition of pyrogenic cytokines release. In the meantime, our study

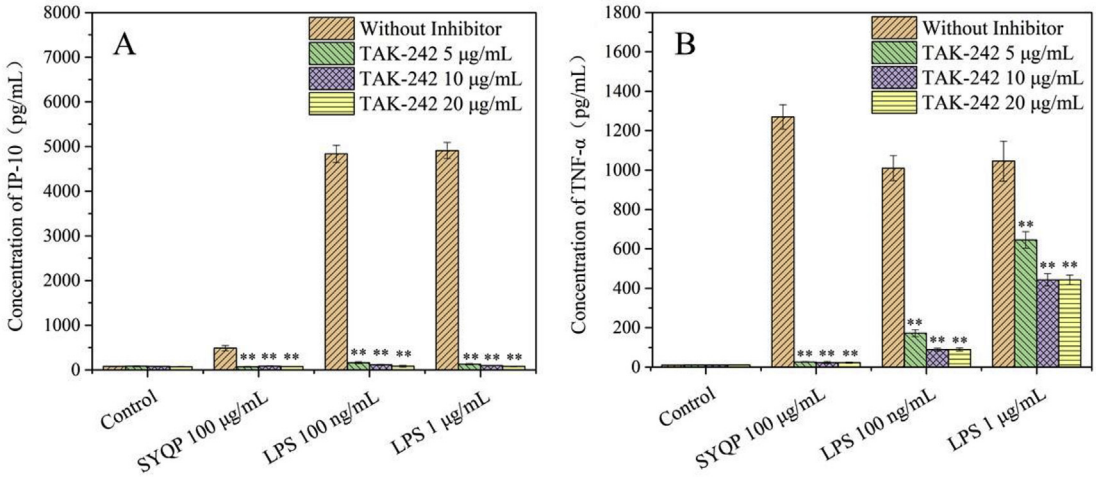

Fig. 5. The effect of SYQP on the cytokines secretion of THP-1 treated by TAK-242 inhibitor (A) effect on the secretion of IP-10; (B) effect on the secretion of TNF-α. **indicated very significant difference from the group without inhibitor, $P < 0.01$.

Table 5
Effect of SYQP on serum cytokines in lipopolysaccharide (LPS) inflammatory model.

Group	Dose (mg/kg)	IL-6 (pg/mL)	IL-10 (pg/mL)	IFN-γ (pg/mL)	TNF-α (pg/mL)	IL-12 (pg/mL)
Normal	–	4.79 ± 1.05	22.38 ± 6.18	5.20 ± 1.47	20.76 ± 5.28	27.11 ± 6.28
LPS	30	17521.20 ± 952.63[b]	257.73 ± 34.50[b]	922.72 ± 256.13[b]	1181.83 ± 251.06[b]	71.76 ± 8.18[b]
SYQP i.p.	150	15192.72 ± 2006.26[bc]	177.13 ± 33.07[bd]	8.75 ± 1.61[bd]	69.90 ± 7.40[bd]	69.09 ± 15.00[b]
SYQP i.g.	150	62.87 ± 12.23[bd]	62.23 ± 5.53[bd]	8.52 ± 1.20[bd]	28.43 ± 3.83[ad]	65.82 ± 11.82[b]
SYQP + LPS	150 + 30	14977.74 ± 2221.13[bd]	174.88 ± 30.90[bd]	10.78 ± 2.50[bd]	1056.34 ± 203.86[b]	67.15 ± 17.61[b]
LPS + SYQP	30 + 150	16119.73 ± 2115.19[bd]	239.26 ± 66.89[b]	111.70 ± 38.94[bd]	1214.50 ± 172.35[b]	62.19 ± 19.27[b]

Results are represented as means ± SD (n = 10).
[a] Indicated significant difference from the normal group, $P < 0.05$.
[b] Indicated very significant difference from the normal group, $P < 0.01$.
[c] Indicated significant difference from the LPS group, $P < 0.05$.
[d] Indicated very significant difference from the LPS group, $P < 0.01$.

showed a significant inhibition rate of 39.9% to H22 tumor in mice model administrated with 200 mg/kg SYQP. The spleen index, thymus index and splenocyte proliferation was found to be proportional to the application of the SYQP, indicating the activation of the immune function by polysaccharides. The stimulated production of cytokines including IP-10 and TNF-α by SYQP and LPS were reduced after the TLR4 inhibitor TAK 242 was added, indicating that both SYQP and LPS stimulate the production of cytokines via TLR4. A further study revealed that the administration of SYQP could stimulate the cytokines production and reduce the serum cytokine levels cause by LPS, which indicated that SYQP may compete with TLR4 in interacting with TLR4 to regulate the production of cytokines. Therefore, our results suggested that the antitumor activities of SYQP were not achieved by the apoptosis of tumor cells but accomplished by its immunoregulatory activity of polysaccharides. This study would provide a basis for developing SYQP as an alternative and complementary agent for tumor and hyperthermia therapy. Elucidating detailed structure and mechanisms of its antipyretic and antitumor activities would be important subjects for further investigation.

Author contributions

Bingqi Zhu and Chaodong Qian collected data, analysed results and wrote manuscript. Fangmei Zhou and Jingjing Guo prepared polysaccharides, conducted analytical experiments including infrared spectral analysis and chromatographic analysis. Nipi Chen and Chenxian Gao were responsible for animal experiments. Bo Jin performed spleen lymphocyte proliferation assay and measurement of cytokines. Zhishan Ding designed experiments and provided suggestions in the experiment and manuscript writing.

Acknowledgments

This work was supported by Key Research Projects of Zhejiang Traditional Chinese Medicine (Grant No. 2019ZZ009); Zhejiang Medical Science and Technology Project (Grant No. 2020RC084, 2017KYB498); National Natural Science Foundation of China (Grant No. 81673672).

References

Ataŏglu, H., Dŏgan, M.D., Mustafa, F., Akarsu, E.S., 2000. Candida albicans and Saccharomyces cerevisiae cell wall mannans produce fever in rats: role of nitric oxide and cytokines. Life Sci. 67 (18), 2247–2256.
Baugh, J.A., Bucala, R., 2001. Mechanisms for modulating TNF alpha in immune and inflammatory disease. Curr. Opin. Drug Discov. Dev 4 (5), 635–650.
Blumenkrantz, N., Asboe-Hansen, G., 1973. New method for quantitative determination of uronic acids. Anal. Biochem. 54 (2), 484–489.
Chen, H., Sun, J., Liu, J., Gou, Y., Zhang, X., Wu, X., Sun, R., Tang, S., Kan, J., Qian, C., Zhang, N., Jin, C., 2019b. Structural characterization and anti-inflammatory activity of alkali-soluble polysaccharides from purple sweet potato. Int. J. Biol. Macromol. 131, 484–494.
Chen, W., Zheng, R., Baade, P.D., Zhang, S., Zeng, H., Bray, F., Jemal, A., Yu, X.Q., He, J., 2016. Cancer statistics in China, 2015. Ca - Cancer J. Clin. 66 (2), 115–132.
Chen, X., Tao, L., Ru, Y., Weng, S., Chen, Z., Wang, J., Guo, L., Lin, Z., Pan, W., Qiu, B., 2019a. Antibacterial mechanism of Tetrastigma hemsleyanum Diels et Gilg's polysaccharides by metabolomics based on HPLC/MS. Int. J. Biol. Macromol. 140, 206–215.
Chu, Q., Jia, R., Chen, M., Li, Y., Yu, X., Wang, Y., Chen, W., Ye, X., Liu, Y., Jiang, Y., Zheng, X., 2019. Tetrastigma hemsleyanum tubers polysaccharide ameliorates LPS-induced inflammation in macrophages and Caenorhabditis elegans. Int. J. Biol. Macromol. 141, 611–621.
Dangarembizi, R., Erlwanger, K.H., Rummel, C., Roth, J., Madziva, M.T., Harden, L.M., 2018. Brewer's yeast is a potent inducer of fever, sickness behavior and inflammation within the brain. Brain Behav. Immun. 68, 211–223.
Du, S., Xiang, T., Song, Y., Huang, L., Sun, Y., Han, Y., 2015. Transgenic hairy roots of Tetrastigma hemsleyanum: induction, propagation, genetic characteristics and medicinal components. Plant Cell Tissue Organ Cult. 122 (2), 373–382.
Dubois, M., Gilles, K.A., Hamilton, J.K., Rebers, P.A., Smith, F., 1956. Colorimetric method for determination of sugars and related substances. Anal. Chem. 28 (3), 350–356.
Fan, S., Yu, G., Nie, W., Jin, J., Chen, L., Chen, X., 2018. Antitumor activity and underlying mechanism of Sargassum fusiforme polysaccharides in CNE-bearing mice. Int. J. Biol. Macromol. 112, 516–522.
Feng, Z., Hao, W., Lin, X., Fan, D., Zhou, J., 2014. Antitumor activity of total flavonoids from Tetrastigma hemsleyanum Diels et Gilg is associated with the inhibition of regulatory T cells in mice. OncoTargets Ther. 7, 947–956.
Guo, W., Yang, Z., Hou, Z., Hou, Z., Qi, Z., Sun, Y., Ding, X., Ma, K., Hu, S., Hu, J., 2019. A comprehensive review of a Chinese folk herbal species tetrastigmae hemsleyanum with multiplicity of pharmacological effects. Chin. Tradit. Med. J. 1 (2), 1–19.
Hu, N., Wang, C., Dai, X., Zhou, M., Gong, L., Yu, L., Peng, C., Li, Y., 2020. Phillygenin inhibits LPS-induced activation and inflammation of LX2 cells by TLR4/MyD88/NF-κB signaling pathway. J. Ethnopharmacol. 248, 112361.
Huang, M., Wang, F., Zhou, X., Yang, H., Wang, Y., 2015. Hypoglycemic and hypolipidemic properties of polysaccharides from Enterobacter cloacae Z0206 in KKAy mice. Carbohydr. Polym. 117, 91–98.
Jiang, S., Qiu, L., Li, Y., Li, L., Wang, X., Liu, Z., Guo, Y., Wang, H., 2016. Effects of Marsdenia tenacissima polysaccharide on the immune regulation and tumor growth in H22 tumor-bearing mice. Carbohydr. Polym. 137, 52–58.
Jiao, R., Liu, Y., Gao, H., Xiao, J., So, K.F., Jiao, R., Liu, Y., Gao, H., Xiao, J., So, K.F., 2016. The anti-oxidant and antitumor properties of plant polysaccharides. Am. J. Chin. Med. 44, 463–488 03.
Jin, M., Zhao, K., Huang, Q., Xu, C., Shang, P., 2012. Isolation, structure and bioactivities of the polysaccharides from Angelica sinensis (Oliv.) Diels: a review. Carbohydr. Polym. 89 (3), 713–722.
Jin, W., Zhang, W., Liu, G., Yao, J., Shan, T., Sun, C., Zhang, Q., 2017. The structure-activity relationship between polysaccharides from Sargassum thunbergii and antitumor activity. Int. J. Biol. Macromol. 105, 686–692.
Liu, D., Cao, G., Han, L., Ye, Y., SiMa, Y., Ge, W., 2016. Flavonoids from Radix Tetrastigmae inhibit TLR4/MD-2 mediated JNK and NF-κB pathway with anti-inflammatory properties. Cytokine 84, 29–36.
Liu, J., Wen, X.-y., Zhang, X.-q., Pu, H.-m., Kan, J., Jin, C.-h., 2015a. Extraction, characterization and in vitro antioxidant activity of polysaccharides from black soybean. Int. J. Biol. Macromol. 72, 1182–1190.
Liu, J., Willför, S., Xu, C., 2015b. A review of bioactive plant polysaccharides: biological activities, functionalization, and biomedical applications. Bioact. Carbohydr. Diet. Fibre 5 (1), 31–61.
Liu, N., Dong, Z., Zhu, X., Xu, H., Zhao, Z., 2018. Characterization and protective effect of Polygonatum sibiricum polysaccharide against cyclophosphamide-induced immunosuppression in Balb/c mice. Int. J. Biol. Macromol. 107, 796–802.
Liu, Y.-J., Du, J.-L., Cao, L.-P., Jia, R., Shen, Y.-J., Zhao, C.-Y., Xu, P., Yin, G.-J., 2015c. Anti-inflammatory and hepatoprotective effects of Ganoderma lucidum polysaccharides on carbon tetrachloride-induced hepatocyte damage in common carp (Cyprinus carpio L.). Int. Immunopharm. 25 (1), 112–120.
Long, T., Liu, Z., Shang, J., Zhou, X., Yu, S., Tian, H., Bao, Y., 2018. Polygonatum sibiricum polysaccharides play anti-cancer effect through TLR4-MAPK/NF-κB signaling pathways. Int. J. Biol. Macromol. 111, 813–821.
Lv, X., Wang, P., Chen, J., Ye, J., 2014. Effect of Sanyeqing Sanjie Kang' ai formula on pathological complete response rates in triple-negative breast cancer patients

undergoing neoadjuvant chemotherapy. J. Tradit. Chin. Med. 55 (23), 2016–2019.
Meng, X., Liang, H., Luo, L., 2016. Antitumor polysaccharides from mushrooms: a review on the structural characteristics, antitumor mechanisms and immunomodulating activities. Carbohydr. Res. 424, 30–41.
Pingsusaen, P., Kunanusorn, P., Khonsung, P., Chiranthanut, N., Panthong, A., Rujjanawate, C., 2015. Investigation of anti-inflammatory, antinociceptive and antipyretic activities of Stahlianthus involucratus rhizome ethanol extract. J. Ethnopharmacol. 162, 199–206.
Roy, R., Ud Daula, A.F.M.S., Akter, A., Sultana, S., Barek, M.A., Liya, I.J., Basher, M.A., 2019. Antipyretic and anti-nociceptive effects of methanol extract of leaves of Fimbristylis miliacea in mice model. J. Ethnopharmacol. 243, 112080.
Ru, Y., Chen, X., Wang, J., Guo, L., Lin, Z., Peng, X., Qiu, B., 2019a. Polysaccharides from Tetrastigma hemsleyanum Diels et Gilg: extraction optimization, structural characterizations, antioxidant and antihyperlipidemic activities in hyperlipidemic mice. Int. J. Biol. Macromol. 125, 1033–1041.
Ru, Y., Chen, X., Wang, J., Guo, L., Lin, Z., Peng, X., Qiu, B., Wong, W.-L., 2019b. Structural characterization, hypoglycemic effects and mechanism of a novel polysaccharide from Tetrastigma hemsleyanum Diels et Gilg. Int. J. Biol. Macromol. 123, 775–783.
Shao, P., Shao, J., Han, L., Lv, R., Sun, P., 2015. Separation, preliminary characterization, and moisture-preserving activity of polysaccharides from Ulva fasciata. Int. J. Biol. Macromol. 72, 924–930.
Sun, Y., Hui, Q., Chen, R., Li, H., Peng, H., Chen, F., Deng, Z., 2018. Apoptosis in human hepatoma HepG2 cells induced by the phenolics of Tetrastigma hemsleyanum leaves and their antitumor effects in H22 tumor-bearing mice. J. Funct. Foods 40, 349–364.
Sun, Y., Li, H., Hu, J., Li, J., Fan, Y.-w., Liu, X.-r., Deng, Z.-y., 2013. Qualitative and quantitative analysis of phenolics in Tetrastigma hemsleyanum and their antioxidant and antiproliferative activities. J. Agric. Food Chem. 61 (44), 10507–10515.
Sun, Y., Tsao, R., Chen, F., Li, H., Wang, J., Peng, H., Zhang, K., Deng, Z., 2017. The phytochemical composition, metabolites, bioavailability and in vivo antioxidant activity of Tetrastigma hemsleyanum leaves in rats. J. Funct. Foods 30, 179–193.
Teotino, U.M., Friz, L.P., Gandini, A., Bella, D.D., 1963. Thio derivatives of 2,3-dihydro-4H-1,3-benzoxazin-4-one. Synthesis and pharmacological properties. J. Med. Chem. 6 (3), 248–250.
Tian, H., Liu, Z., Pu, Y., Bao, Y., 2019. Immunomodulatory effects exerted by Poria Cocos polysaccharides via TLR4/TRAF6/NF-κB signaling in vitro and in vivo. Biomed. Pharmacother. 112, 108709.
Timilsena, Y.P., Adhikari, R., Kasapis, S., Adhikari, B., 2016. Molecular and functional characteristics of purified gum from Australian chia seeds. Carbohydr. Polym. 136, 128–136.
Wang, C., Feng, L., Su, J., Cui, L., Dan, L., Yan, J., Ding, C., Tan, X., Jia, X., 2017. Polysaccharides from Epimedium koreanum Nakai with immunomodulatory activity and inhibitory effect on tumor growth in LLC-bearing mice. J. Ethnopharmacol. 207, 8–18.
Wang, C.Y., Lee, J.S., Su, X.D., Li, H.X., Lee, S.K., Wang, H.-S., Kim, Y.H., Yang, S.Y., 2018. Three new constituents from the aerial parts of Tetrastigma hemsleyanum. Phytochem. Lett. 27, 25–29.
Wang, L., Li, Y., Zhu, L., Yin, R., Wang, R., Luo, X., Li, Y., Li, Y., Chen, Z., 2016. Antitumor activities and immunomodulatory of rice bran polysaccharides and its sulfates in vitro. Int. J. Biol. Macromol. 88, 424–432.
Wang, Y.-q., Mao, J.-b., Zhou, M.-q., Jin, Y.-w., Lou, C.-h., Dong, Y., Shou, D., Hu, Y., Yang, B., Jin, C.-y., Shi, H.-c., Zhao, H.-j., Wen, C.-p., 2019. Polysaccharide from Phellinus Igniarius activates TLR4-mediated signaling pathways in macrophages and shows immune adjuvant activity in mice. Int. J. Biol. Macromol. 123, 157–166.
Wright, S., Ramos, R., Tobias, P., Ulevitch, R., Mathison, J., 1990. CD14, a receptor for complexes of lipopolysaccharide (LPS) and LPS binding protein. Science 249 (4975), 1431–1433.
Wu, Y.-G., Wang, K.-W., Zhao, Z.-R., Zhang, P., Liu, H., Zhou, G.-J., Cheng, Y., Wu, W.-J., Cai, Y.-H., Wu, B.-L., Chen, F.-Y., 2019. A novel polysaccharide from Dendrobium devonianum serves as a TLR4 agonist for activating macrophages. Int. J. Biol. Macromol. 133, 564–574.
Xie, X., Wang, J., Zhang, H., 2015. Characterization and antitumor activities of a water-soluble polysaccharide from Ampelopsis megalophylla. Carbohydr. Polym. 129, 55–61.
Xiong, Y., Wu, X., Rao, L., 2015. Tetrastigma hemsleyanum (Sanyeqing) root tuber extracts induces apoptosis in human cervical carcinoma HeLa cells. J. Ethnopharmacol. 165, 46–53.
Xu, G.-Y., Liao, A.-M., Huang, J.-H., Zhang, J.-G., Thakur, K., Wei, Z.-J., 2019. Evaluation of structural, functional, and anti-oxidant potential of differentially extracted polysaccharides from potatoes peels. Int. J. Biol. Macromol. 129, 778–785.
Ye, C.-L., Liu, X.-G., 2015. Extraction of Flavonoids from Tetrastigma hemsleyanum Diels et Gilg and Their Antioxidant Activity. J. Food Process. Preserv. 39 (6), 2197–2205.
Yu, Y., Shen, M., Song, Q., Xie, J., 2018. Biological activities and pharmaceutical applications of polysaccharide from natural resources: a review. Carbohydr. Polym. 183, 91–101.
Zhao, L., Li, M., Sun, K., Su, S., Geng, T., Sun, H., 2019. Hippophae rhamnoides polysaccharides protect IPEC-J2 cells from LPS-induced inflammation, apoptosis and barrier dysfunction in vitro via inhibiting TLR4/NF-κB signaling pathway. Int. J. Biol. Macromol.
Zhao, Y., Sun, H., Ma, L., Liu, A., 2017. Polysaccharides from the peels of Citrus aurantifolia induce apoptosis in transplanted H22 cells in mice. Int. J. Biol. Macromol. 101, 680–689.
Zheng, Y.-F., Zhang, Q., Liu, X.-M., Ma, L., Lai, F., 2016. Extraction of polysaccharides and its antitumor activity on Magnolia kwangsiensis Figlar & Noot. Carbohydr. Polym. 142, 98–104.
Zheng, Y., Wang, W.-d., Li, Y., 2015. Antitumor and immunomodulatory activity of polysaccharide isolated from Trametes orientalis. Carbohydr. Polym. 131, 248–254.
Zhong, L.-r., Zheng, J., Sun, Q., Wei, K., Hu, Y., 2016. Radix Tetrastigma hemsleyani flavone inhibits proliferation, migration, and invasion of human lung carcinoma A549 cells. OncoTargets Ther. 9, 635–641.
Zong, S., Li, J., Yang, L., Huang, Q., Ye, Z., Hou, G., Ye, M., 2018. Synergistic antitumor effect of polysaccharide from Lachnum sp. in combination with cyclophosphamide in hepatocellular carcinoma. Carbohydr. Polym. 196, 33–46.